Excitonic photoluminescence quenching by impact ionization of excitons and donors in GaAs/$Al_{0.35}Ga_{0.65}As$ quantum wells with an in-plane electric field

J. Kundrotas, G. Valušis, A. Čėsna,* A. Kundrotaitė, A. Dargys, A. Sužiedėlis, J. Gradauskas, and S. Ašmontas
Semiconductor Physics Institute, A. Goštauto 11, LT-2600 Vilnius, Lithuania

K. Köhler
Fraunhofer-Institut für Angewandte Festkörperphysik, D-79108 Freiburg, Germany
(Received 1 February 2000)

We present a detailed experimental study on photoluminescence quenching due to exciton and donor impact ionization by accelerated electrons under an in-plane nanosecond duration electric field created in GaAs/$Al_{0.35}Ga_{0.65}As$ quantum wells. From the photoluminescence transients measured by the time-correlated single-photon counting technique, we have determined the experimental conditions under which donor impact ionization can have an influence on quenching of the excitonic photoluminescence. The coefficient of two-dimensional exciton impact ionization has been estimated; its dependences on the applied electric field, lattice temperature, and width of the quantum wells are given.

I. INTRODUCTION

The ionization of intrinsic and extrinsic defects in bulk semiconductors and quantum wells (QWs) can be caused by thermal vibrations of atoms (so-called thermal ionization), by a photon absorption, or by free charge carriers due to Auger process. In the latter case of special interest is the impact ionization (II) in high electric fields. The energy which is required for ionization of defects is usually smaller than the band gap of the materials studied. Up to now the phenomenon of II has revealed interesting basic physics and led to a number of applications (see review on II in Ref. 1). However, the situation of impact ionization in nanostructures differs strongly from the well-documented case in bulk semiconducting materials. For example, in two-dimensional (2D) nanostructures the presence or absence of the impact ionization processes of impurities and excitons is defined, in principle, by the fact whether electric field is applied *along* the axis of the structure growth or it is oriented *in-parallel* to the nanostructure layers. In the first case, the electric field in QWs induces the quantum-confined Stark effect, i.e., polarization of electron-hole pairs within the wells.[2–4] At high electric fields, exceeding 50 kV/cm, the excitonic field ionization predominates.[5,6] In superlattices (SLs) with strong interwell coupling the situation is similar although excitons are ionized at lower electric fields, usually lying within so-called miniband field regime.[7] The duration of such processes is within the picosecond and subpicosecond time scale for the electric fields in the order of a few kV/cm.[8] Thus, this geometry eliminates the II process in the QWs and SLs, since 2D carriers cannot be accelerated by the electric field to high energies due to carrier confinement by layers.

If applied electric field is *parallel* to the layers (case of in-plane electric field), the general physical picture is quite similar to that occurring in bulk materials:[1] Free charge carriers can be accelerated by electric fields to kinetic energies high enough to ionize defects and to destroy excitons by the direct impact. Since exciton binding energies in quantum wells are of the order of 10–15 meV, the II should be observed at comparatively low electric fields. Weman *et al.*[9] have studied exciton and donor impact ionization processes in $Al_xGa_{1-x}As$/(*n*-type GaAs):Si quantum wells in dc in-plane electric field by low-temperature luminescence. The authors observed sharp thresholds in the quenching of the luminescence from the free and bound excitons at fields near a few tens of V/cm accompanied by a sharp increase in the current. As a responsible mechanism, the exciton II by the free carriers heated in the electric field was suggested.

However, to the best of our knowledge, the experimental study of *transient processes* under impact ionization conditions in a quantum well is still lacking.

In the present paper we report on research of photoluminescence (PL) transients caused by the electric field applied parallel to the layers of GaAs/$Al_{0.35}Ga_{0.65}As$ quantum wells at temperatures that are close to liquid nitrogen and liquid helium temperatures. Combining the time-correlated single-photon counting technique and electrical pulses of nanosecond duration, we were able to resolve experimentally the exciton and donor II processes in the time domain. The PL transients were modeled by using a set of coupled rate equations.

II. SAMPLES AND EXPERIMENTAL TECHNIQUE

The PL experiments were performed on samples containing three QWs of GaAs/$Al_{0.35}Ga_{0.65}As$ with a width L_w of 20, 10, and 5 nm. These structures were grown by molecular beam epitaxy on the semi-insulating substrate. Ohmic contacts were formed by evaporating parallel strips of Au-Ni-Ge with the subsequent annealing in the H_2 atmosphere at $\sim$450°C for 2 min. The distance between the strips was either 0.5 mm or 1 mm. Nanosecond duration or dc electric field was applied in parallel direction to the layers of the QWs. The strength of the electric field was estimated by dividing the applied voltage by the contact spacing.

The surface of the samples was illuminated continuously with an argon-ion laser with an energy of 2.38–2.75 eV, i.e., carriers were excited in the barriers and in the wells far

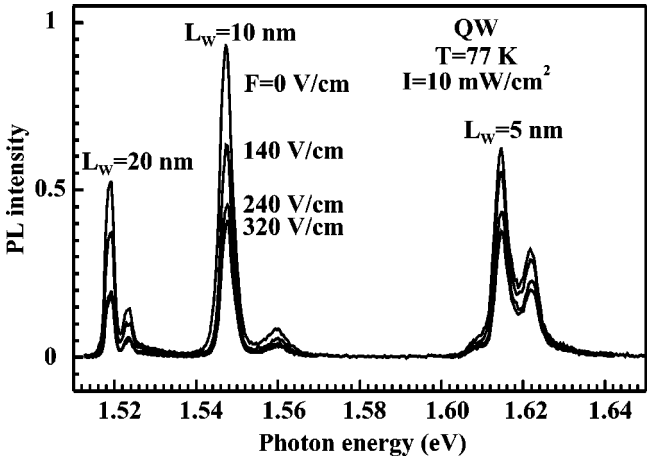

FIG. 1. Stationary PL spectra of GaAs/$Al_{0.35}Ga_{0.65}As$ QWs of $L_w = 5$, 10, and 20 nm at liquid nitrogen temperature at various strengths of dc electric field.

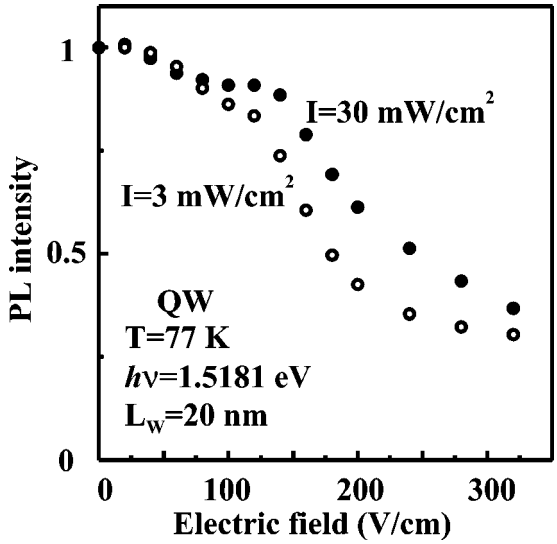

FIG. 2. Dependence of the stationary PL intensity on the electric field strength at two illumination intensities of 20 nm GaAs/$Al_{0.35}Ga_{0.65}As$ QW.

above the resonances. The illumination spot covered all the area between the contacts. Typical excitation intensity I on the illuminated surface varied from 1 to 100 mW/cm^2.

For the excitation and collection of the emission by the sample, the light optical fibers were used. The collected light was dispersed by a monochromator and detected by a photomultiplier. The stationary photoluminescence and time-correlated single-photon counting techniques were used in the detection system.

The fibers along with the electrical cables for propagation of nanosecond voltage pulses were mounted inside a special insert stick, one end of which was immersed in helium or nitrogen storage dewar. To avoid multiple voltage reflections in the cables and in order to support constant amplitude of voltage over the sample during breakdown, the sample was shunted with a 50 Ω resistor. Experiments were performed at liquid helium and at liquid nitrogen temperatures.

III. EXPERIMENTAL RESULTS AND DISCUSSION

A. PL quenching at dc electric fields

Figure 1 shows the stationary PL spectra of studied QWs at liquid nitrogen temperature and at different dc electric fields. Three groups of transitions associated with excitons in three QWs of different widths are clearly visible. Analysis of transition energies suggests that the strongest PL lines in luminescence doublets are due to luminescence of heavy-hole excitons.[10,11] As for the origin of their weaker satellites, we attribute them to the excited states of relevant heavy-hole excitons.[12]

It is seen that in all cases the application of dc electric field decreases the PL intensity of excitonic lines. Calculations show[13] that in electric fields from 100 V/cm to 400 V/cm the mean electron energy varies from 12 to 20 meV. Since the exciton binding energy in QWs of 20 to 5 nm width is from 7 to 12 meV, it is reasonable to think that II of excitons by electrons heated in in-plane electric fields can be assumed to be responsible for the PL quenching.

Excitonic PL intensity versus dc electric field F under different illumination intensities for the 20 nm well is plotted in Fig. 2. (The dependences for other QWs are similar and therefore not shown here.) It is seen that the decrease of the PL intensity is larger at low excitation levels. The physical reasons for this effect cannot be deduced from the stationary PL spectra alone. As will be shown later, only transient PL processes in pulsed electric field allow us to explain this.

Before proceeding to the transient PL research, we would like to make some remarks on the stationary PL spectra measured at liquid helium temperature and depicted in Fig. 3. In comparison to the data at liquid nitrogen temperature, the spectra at 4.2 K have an additional feature—the spectral line shifts with the increase of electric field strength. Especially, the effect is pronounced for the narrowest well.

We attribute this observation to the delocalization of trapped to interface state 2D excitons[14–16] by the electric field. In more detail, the physical picture is the following: Free carriers heated by electric field can interact with excitons causing either impact ionization or suppression of trapping of excitons to interface states. If one assumes that total trap density does not depend on the width of the well, in the

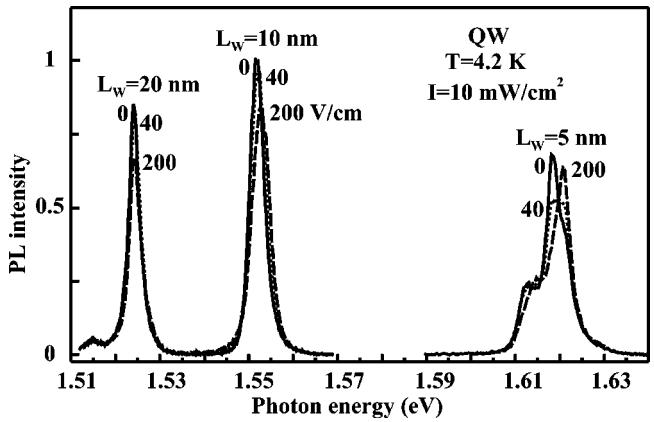

FIG. 3. Stationary PL spectra of GaAs/$Al_{0.35}Ga_{0.65}As$ QWs of $L_w = 5$,10, and 20 nm at liquid helium temperature in the absence of electric field and at in-plane electric fields of 40 and 200 V/cm.

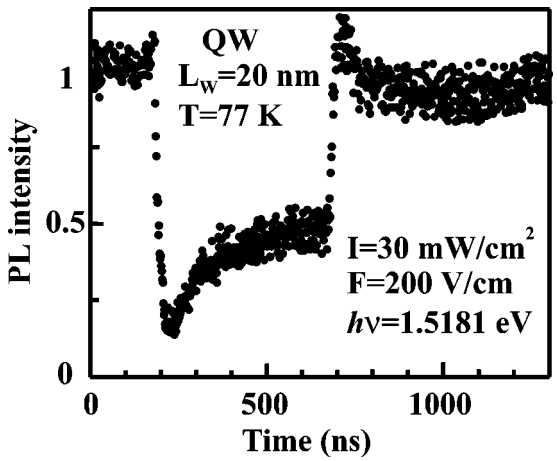

FIG. 4. The transient PL of 20 nm GaAs/$Al_{0.35}Ga_{0.65}As$ QW in arbitrary units. The electric field was applied from 170 to 670 ns.

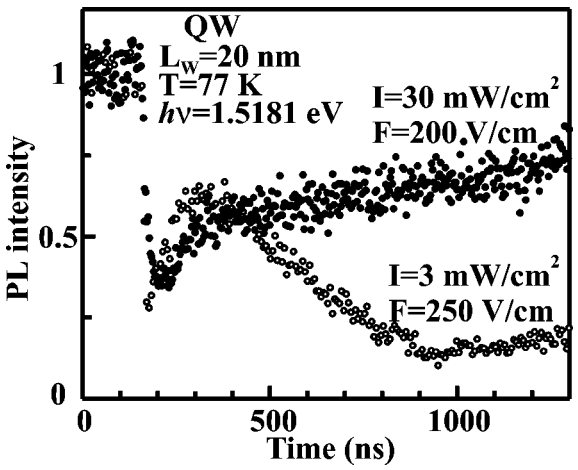

FIG. 5. The transient PL of 20 nm GaAs/$Al_{0.35}Ga_{0.65}As$ QW at two illumination intensities. The electric field was switched on at $t=150$ ns.

narrower well the exciton ''feels'' interface roughness more strongly. Consequently, one expects that the narrower the well, the higher the probability of the exciton localization. Therefore, it is reasonable that the spectral shifts due to exciton localization are more pronounced for the narrower well. Furthermore, the narrower the well, the shorter the lifetime of free carriers, thus there is a large probability for carriers to recombine without forming excitons. As a result, relatively low PL is detected from the 5 nm well. Another possible explanation of this effect is that the conditions for trapping of new light generated excitons in the electric field is less favorable than in the absence of the field. Due to collisions with the hot carriers, the exciton temperature may be slightly higher than the lattice one. As a consequence, the exciton trapping by the interface will be suppressed.

The relation of these spectral shifts with the exciton delocalization was confirmed also by varying lattice temperature: As expected, experiments indicated the disappearance of spectral shifts at lattice temperatures of 25–40 K.

Thus, the application of the dc electric field quenches the excitonic PL lines due to II of the excitons by field-accelerated electrons in QWs. However, the stationary luminescence provides limited information on the evolution of II process. Therefore, to get an insight into transient processes, we have applied a somewhat nonconventional approach: The sample was illuminated by the continuous laser irradiation while electric field pulses of nanosecond duration with leading edge risetime of 300 ps were used to impact-ionize the excitons. This has allowed us to avoid undesirable effects due to current filamentation and to have homogeneous lateral distribution of excitons and free carriers before the II process has been set up.

B. PL transients at nanosecond time scale

The PL transients were measured at various strengths of electric field and intensities of the illumination. A typical PL transient at 77 K for 20 nm width QW is shown in Fig. 4. The electric field was applied in the time interval $t=200-700$ ns. Two characteristic features are clearly visible: The dip in the PL intensity in the leading edge of the electrical pulse and the overshoot after the electric field was switched off. PL analysis with the help of rate equations, as we shall see, indicates that these features are present when the nonradiative recombination time of free carriers τ_n is longer than the radiative recombination time of exciton τ_X. We observed that the characteristic quenching time of the PL intensity is strongly sensitive to the applied electric field. For instance, at the 0.1–0.9 level of the leading edge the transient time of PL quenching is about 100 ns at 10 V/cm, while it is close to 3 ns at 500 V/cm. It is worth noting that the PL quenching is observable in the fields as low as 5 V/cm. In Sec. IV it will be shown that the observed strong dependence of the transient time on electric field strength is associated with the strong (exponential) dependence of the exciton II coefficient on 2D free electron temperature.

The decrease of illumination intensity drastically changes an overall picture of the PL transients, as is evidenced by Fig. 5 and Fig. 6, where normalized PL transients at two different illumination intensities under step-shaped electric field are presented for 20 nm and 10 nm QWs, respectively. Only the transients after application of the electric field are shown in the figures. It is evident that some other processes become important, depending on illumination intensity. At 30 mW/cm^2 the PL evolution in Fig. 5 is similar to that in

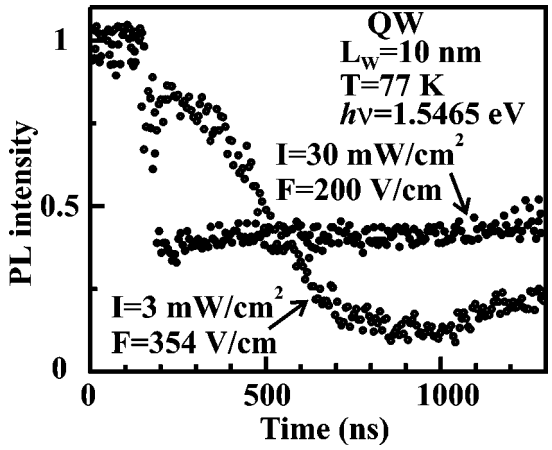

FIG. 6. The transient PL of 10 nm GaAs/$Al_{0.35}Ga_{0.65}As$ QW at two illumination intensities. Note the absence of the fast transient at higher intensities in comparison to Fig. 5.

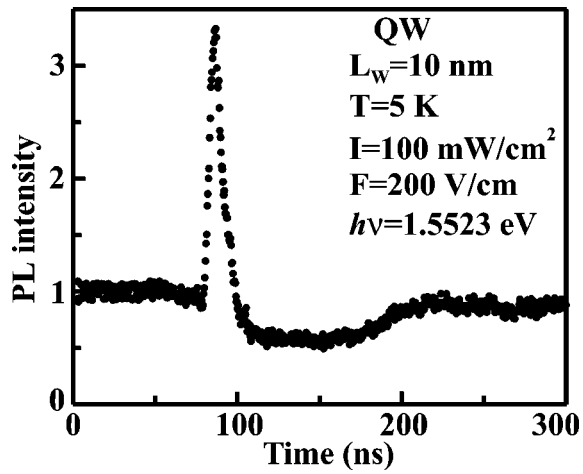

FIG. 7. The flash in excitonic PL for 10 nm $GaAs/Al_{0.35}Ga_{0.65}As$ QW under electric field pulse of 120 ns duration at $T=5$ K.

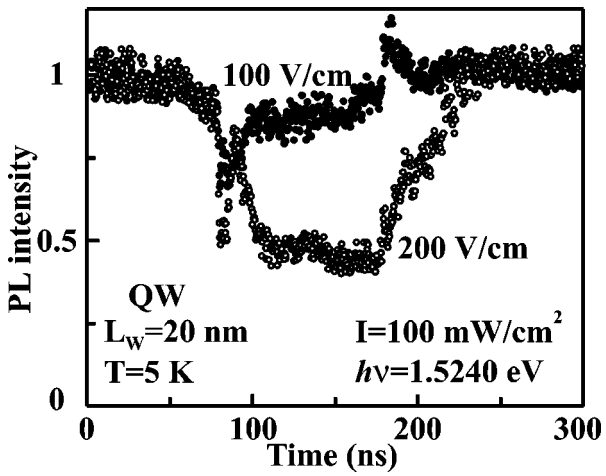

FIG. 9. The evolution of excitonic PL for 20 nm $GaAs/Al_{0.35}Ga_{0.65}As$ QW under 120 ns electric field pulse of 100 V/cm and 200 V/cm strength. $T=5$ K.

Fig. 4, however when illumination is reduced to the 3 mW/cm^2 level, the character of the PL transient has changed. Now, two processes can be discriminated: The first, which is in a hundred nanosecond time scale, is quite similar to that depicted in Fig. 4. The second process appears approximately after 500 ns and dominates up to 1000 ns. We identify the fast process as II of excitons by the electric field accelerated carriers, while the origin of the slower one is thought to be related with the II of residual impurities. At first glance it might appear that the excitonic PL should not be sensitive to impurity II. These processes, however, are indirectly related through the role of nonequilibrium holes as illustrated earlier in bulk GaAs (Ref. 17): Before application of the electric field, the electrons and holes excited by laser illumination almost completely neutralize charged donors and compensating acceptors. Under intense illumination, the influence of residual impurities on II of excitons is not important. The circumtances change at low illumination intensity, when concentration of excitons is comparable or even lower than the concentration of residual impurities in QWs. In the presence of electric field, the II of neutral donors increases the concentration of electrons, which effectively recombine with holes through the acceptor level. As a consequence, a decrease in hole concentration diminishes exciton concentration, since exciton concentration is proportional to the product of electron and hole concentrations. In that way the II of donors manifests itself in exciton PL spectra, and the transients show that this process is slower than the exciton impact ionization.

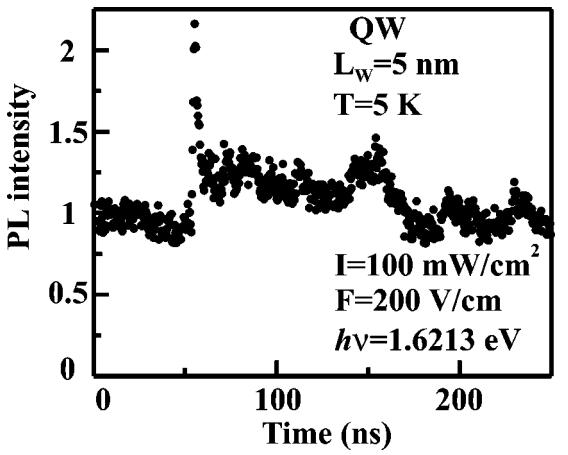

FIG. 8. The evolution of excitonic PL for 5 nm $GaAs/Al_{0.35}Ga_{0.65}As$ QW under electric field pulse of 120 ns duration at $T=5$ K.

On the basis of these experimental findings, it can be inferred that the interpretation of excitonic spectra in dc fields is rather complicated since two II processes (impact ionization of excitons and of residual donors), both being caused by field accelerated electrons, overlap in time. Therefore, these processes can be discriminated in time domain only from PL transients induced by the pulses of the electric field of nanosecond duration.

The decrease in lattice temperature reveals new additional features in the PL transients, in particular for narrower wells. Figure 7 displays the PL transient taken at temperature close to that of liquid helium. It is seen that the 10 nm well produces the PL flash at the leading egde of the electrical pulse. For the 5 nm well (Fig. 8), the flash in the PL is shorter. As we shall see in Sec. IV, the dependence of the flash reflects the competition between exciton and donor impact ionization processes (cf. the solid curve in Fig. 11). The flat part after the flash is due to an increase of the PL at 1.6213 eV energy and is associated with trapped to interface state exciton delocalization and PL peak shift to higher energies, as was demonstrated in case of the dc electric fields in Fig. 3. In contrast to the narrower well, the PL transient of the 20 nm well (Fig. 9) at 5 K is similar to that at liquid nitrogen temperature. Figure 9 clearly displays that in addition to the pulsed illumination intensity technique, which is more common in transient PL experiments, the pulsed electric field can be used with success as well to govern the PL evolution processes. In Fig. 9 at lower pulsed electric field, the PL transient reproduces the shape observed earlier at 77 K and at higher intensities (Fig. 4). In stronger fields in Fig. 9 as well as at lower illumination intensity in Fig. 4, two processes can be resolved: The fast one caused by exciton II and the slower one which originates from the II of residual donors.

IV. SIMULATION OF THE PHOTOLUMINESCENCE TRANSIENTS

In this section we present theoretical considerations directly illustrating the interpretation of the experimental data in the whole set of the measurements. As a rule, the distribution of particles in a QW generated by a short laser pulse, the photon energy of which is larger than the barrier energy gap, is rather complicated and is related mainly with a nonuniform charge-carrier distribution in the sample. The use of continuous laser illumination significally reduces the nonuniformity due to the diffusion effects, therefore in calculations we neglected all concentration gradients and related phenomena. The good quality of the samples and low background impurity concentration allowed us to ignore deep center trapping effects.[18] Since the studied processes are associated only with the wells, it is reasonable to neglect the particle's nonuniform distribution in the barrier. Thus, under these circumstances, the physical phenomena can be modeled by a system of coupled rate equations for corresponding particle densities in the well.

The following kinds of particles will be included: Free electrons and free holes with concentrations n and p, respectively; neutral and positively ionized donors of concentrations N_D^0 and N_D^+; neutral and negatively ionized compensating acceptors of concentrations N_A^0 and N_A^-; excitons with concentration N_X. In the model we assumed that the total residual concentrations of donors and acceptors in QWs are, respectively, $N_D=6\times10^8$ cm^{-2} and $N_A=3\times10^8$ cm^{-2}. Before proceeding further, we turn first to the considerations on the rate coefficients.

(i) *Free electron-hole pair generation in a QW by a laser*. In a general case, electron-hole pairs are generated both in QWs and in the barriers. At the excitation photon energy of 2.4 eV, the absorbtion coefficient α is equal to 10^5 cm^{-1} for GaAs and 6×10^4 cm^{-1} for GaAs/$Al_{0.35}Ga_{0.65}As$.[19] If the light intensity is 10 mW, the generation rate will be $G\approx5\times10^{15}$ cm^{-2}/s. Theoretical and experimental investigations show that the capture of free electrons into the QW occurs within 150–500 ps.[20,21] Since we simulate the process in a nanosecond time scale, we assume that independent of electric field value the same number of light generated carriers is captured into the QWs; therefore, the value $G=1\times10^{16}$ cm^{-2}/s was used in the simulation.

(ii) *Free electron and hole recombination with residual shallow impurities*. Usually, at low temperatures photoexcited electrons and holes nearly completely neutralize the shallow ionized donors and acceptors.[17] Then free electrons recombine with holes bound to an acceptor (so-called e-A transition). The e-A recombination time determined by time-resolved PL measurements in Be-doped $Al_xGa_{1-x}As$/GaAs QWs was found to be $\tau_{eA}\approx30$ ns, while hole trapping by an ionized acceptor was estimated to be shorter than $\tau_h=5$ ps.[22] Therefore, the e-A recombination rate coefficient is equal to $B_{eA}=1/N_A^0\tau_{eA}=0.1$ cm^2/s. For a better fit of the theory and the experimental results, we used the hole-to-acceptor rate coefficient B_A equal to 10 cm^2/s and the electron-to-donor rate coefficient $B_D=1$ cm^2/s.

(iii) *Free electron and hole recombination into free excitons*. The exciton formation coefficient γ determined experimentally ranges from 0.5 up to 14 cm^2/s.[23–25] In general, γ changes with electric field F. For example, in Ge, γ is inversely proportional to F.[26] No measurements of γ have been performed using 2D excitons. Bearing in mind the fact that the binding energies of the exciton and the shallow donor are similar,[27] we used in the calculations the constant value $\gamma=1$ cm^2/s and $B_D=1/N_D^+\tau_n=1$ cm^2/s.

(iv) *Radiative decay of free-excitons*. It is known that the free-exciton radiative recombination time τ_X depends on the width of the QW and follows the linear law with lattice temperature, i.e., $\tau_X=CT$.[28] The coefficient C is found to be 22 ps/K for a 4 nm QW, 32 ps/K for a 12 nm QW, 65 ps/K for an 18 nm QW,[29] and 100 ps/K for $L_w=10$ nm.[30] In our calculations the value of $\tau_X=1$ ns was used. The decay coefficient is defined as $W_X=1/\tau_X$.

(v) *Impact ionization of excitons and shallow impurities*. The II coefficient of excitons A_X depends on the free-carrier distribution function in the QW and the cross section of exciton impact ionization which is a function of QW width.[31] In electric fields, when carriers become hot, the carrier distribution function changes causing a variation of impact ionization coefficient of excitons from small values at low electron temperatures up to 50 cm^2/s at electron temperatures of about 100 K.[32] Since the impact ionization coefficient A_D of shallow donors in a QW is unknown, and the impact ionization of impurities has a critical impact ionization field, in calculations we used the following values: $A_X=10$ cm^2/s and $A_D=0$ at fields lower than critical field $F_c=5$ V/cm and $A_X=10$ cm^2/s and $A_D=1$ cm^2/s for fields $F>F_c$. We neglected here the impact ionization of acceptors because their ionization energy is larger by a factor of 5 than relevant exciton and acceptor energies.

Our calculations were performed for low lattice temperatures, therefore thermal ionization processes have not been included in the simulation model.

We solved the set of four coupled rate equations for free electrons, holes, neutral acceptors, and free excitons,

$$\frac{dn}{dt}=G-nN_D^+B_D-nN_A^0W_{eA}+nN_D^0A_D-np\gamma+nN_XA_X, \tag{1}$$

$$\frac{dp}{dt}=G-pN_A^-B_A-np\gamma+nN_XA_X, \tag{2}$$

$$\frac{dN_A^0}{dt}=pN_A^-B_A-nN_A^0W_{eA}, \tag{3}$$

$$\frac{dN_X}{dt}=np\gamma-N_XW_X-nN_XA_X, \tag{4}$$

by the Runge-Kutta method. The product of N_X and W_X gives the intensity I_X of the excitonic PL.

The concentrations of the remaining acceptors and donors N_A^-, N_D^+, and N_D^0 can be found from the charge-neutrality equation, $n+N_A^-=p+N_D^+$, and noting that the total number of donors, $N_D=N_D^0+N_D^+$, and acceptors, $N_A=N_A^0+N_A^-$, does not change with time:

$$N_A^-=N_A-N_A^0, \tag{5}$$

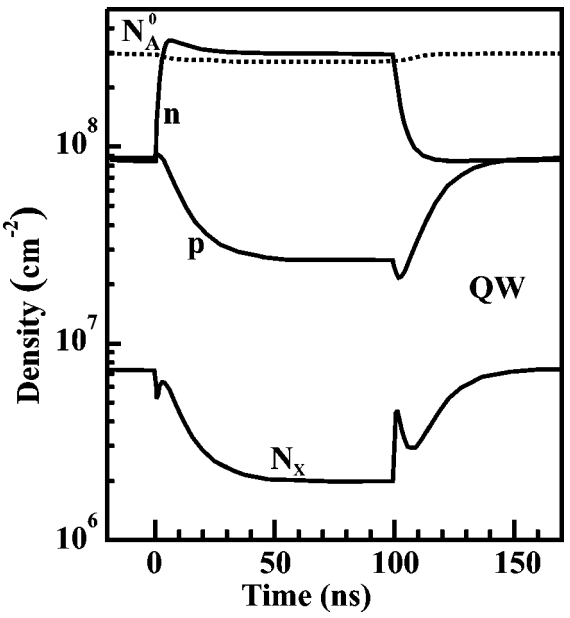

FIG. 10. Calculated transient carrier concentrations. The electric field is switched on at $t=0$ and switched off at $t=100$ ns. N_X, n, and p label exciton, electron, and hole concentrations, respectively. N_A^0 is the neutral acceptor concentration.

$$N_D^+ = n + N_A^- - p, \tag{6}$$

$$N_D^0 = N_D - N_D^+ . \tag{7}$$

Figure 10 depicts some of the solutions obtained with Eqs. (1)–(7) at impurity concentrations of $N_D = 6\times10^8$ cm^{-2} and $N_A = 3\times10^8$ cm^{-2}. The steady–state solutions under continuous laser irradiation served as the initial conditions for Eqs. (1)–(7). In our model it is assumed that only II coefficients depend on the electric field. At times $t<0$ and $t>100$ ns the electric field is absent, therefore the II coefficients for excitons and donors in Eqs. (1)–(4) were equal to zero at these times. The electric field was applied in the time interval $0<t<100$ ns, where $A_X = 10$ cm^{-2}/s and $A_D = 1$ cm^{-2}/s. It is worth noting that the experimentally observed excitonic intensity is directly proportional to exciton concentration.

To understand the behavior of the concentrations presented in Fig. 10 and the time dependence of PL intensity in Fig. 11, we have solved rate equations under three different conditions.

(i) The dotted line in Fig. 11 shows the case when the free-exciton lifetime τ_X is equal to the free-electron lifetime τ_n, i.e., $\tau_X = \tau_n = 1$ ns. As it is seen in Fig. 10, when the impact ionization becomes important, the concentration of excitons begins to decrease, which causes an increase in electron and hole concentrations (experimentally this is evident from the transients under strong illumination in Fig. 6).

(ii) The dashed line in Fig. 11 demonstrates the PL transients when the free-exciton lifetime is less than the free-electron lifetime ($\tau_X = 1$ ns, $\tau_n = 33$ ns). It is clear that the excitonic PL transient has two parts. Initially, after switching on of the electric field, the PL intensity is quenched very fast, but later it begins to grow slowly. The calculated evolution of the PL nicely reproduces transients observed experimentally (Fig. 4 and Fig. 5, strong illumination).

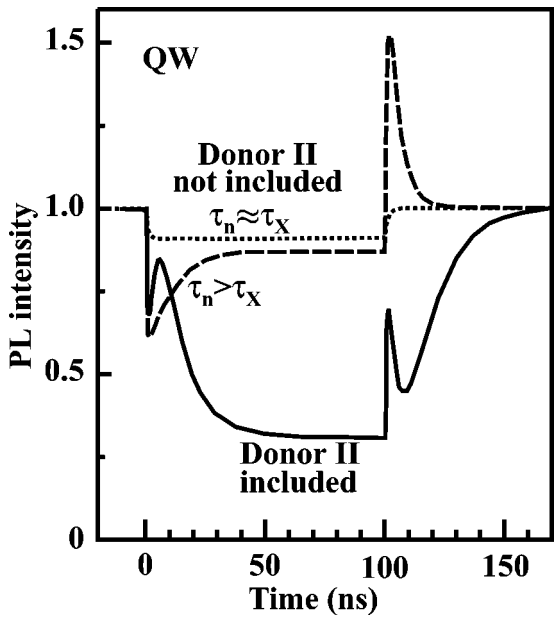

FIG. 11. Simulated exciton PL transient at different conditions. Dotted line, the impact ionization of donors is not included and free exciton lifetime τ_X is equal to free electron lifetime τ_n. Other parameters: $A_D^I = 0$ cm^2/s, $\tau_X = 1$ ns, $\tau_n = 1$ ns; dashed line, the impact ionization is not included, but free exciton lifetime is less than that of free electrons. Other parameters: $A_D^I = 0$ cm^2/s, $\tau_X = 1$ ns, $\tau_n = 33$ ns; solid line, impact ionization of donors is included. Other parameters: $A_D^I = 1$ cm^2/s, $\tau_X = 1$ ns, $\tau_n = 33$ ns.

(iii) The solid curves in Fig. 10 and Fig. 11 show the case when the impact ionization of both excitons and donors is taken into account. More specifically, the coefficients of exciton and donor impact ionization in the presence of electric fields were assumed to be $A_X = 10$ cm^2/s and $A_D = 1$ cm^2/s, respectively, while the free-exciton lifetime τ_X was taken less than the free-electron lifetime τ_n. [These values are reasonable for 20 nm QW (Ref. 33)]. Figures 10 and 11 reveal the following evolution of the QW breakdown process: Before application of the electric field, the electrons and holes generated by a laser completely neutralize the charged donors and acceptors. In the presence of electric fields, the exciton concentration changes due to two competing processes. On the one hand, the field-accelerated electrons ionize the excitons, thus reducing their concentrations. On the other hand, the hot electrons ionizing collisions with the neutral donors favor the opposite process, i.e., exciton formation, because the probability of exciton generation is proportional to the product of free electron and hole concentrations. As a result of the competition of these two processes, the flash forms on the leading edge of the PL transient as seen in Fig. 11. Experimentally this peculiarity was clearly observed in Fig. 5. The comparison of the calculated results and experimental data after switch-off of the field implies that the recovery of the PL is much longer than the calculated one. We suppose that, probably, this discrepancy is related to the omission of the donor-acceptor transitions.[34]

V. EVALUATION OF THE COEFFICIENT OF THE EXCITON IMPACT IONIZATION

Theoretically, the coefficient of impact ionization of excitons is defined[32] as

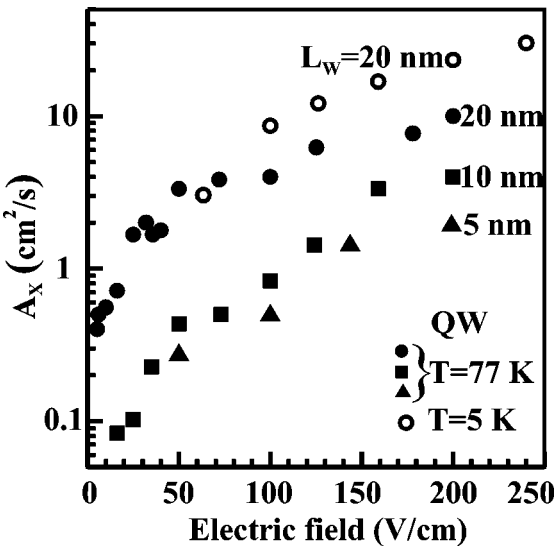

FIG. 12. Coefficient of exciton impact ionization versus the electric field. Dark symbols, $T=77$ K; open circles, $T=5$ K. Numbers 5, 10, and 20 label the width of the GaAs/$Al_{0.35}Ga_{0.65}As$ QWs.

$$A_X=\int_0^\infty f_0(\epsilon)v(\epsilon)\sigma_X(\epsilon)d\epsilon. \tag{8}$$

It is apparent that the II coefficient depends on the carrier disribution function f_0 and II cross section σ_X. In Eq. (8), $v(\epsilon)$ is the velocity of the free electron equal to $v(\epsilon)=\sqrt{2\epsilon/m^*}$, where ϵ is the free-electron energy. One can note that in the definition of II of 2D excitons in QWs by Eq. (8), in comparison to the three-dimensional case the Eq. (8) contains no $\sqrt{\epsilon}$, since in the two-dimensional case the density of states does not depend on energy and is equal to $\rho_{2D}=m^*/\pi\hbar^2$.[35] The cross section is one-dimensional and depends on the exciton type (heavy or light hole) and the sort of charge carriers participating in the II process (electrons, heavy, or light holes).

In Ref. 36, the 3D exciton II coefficient was estimated considering the transient luminescence at the initial time moments, where it was shown that the PL decay curve has the slope $1/\tau=N_{EX}/(N_{0X}\Delta t)$, where N_{0X} is the initial exciton concentration and N_{EX} denotes the exciton concentration in an electric field. If electron concentration n_0 is known, then, as shown in Ref. 36, the coefficient of exciton impact ionization can be found from $A_X=1/(\tau n_0)$.

In this way the obtained A_X values for studied QWs are given in Fig. 12 at an illumination of 30 mW/cm^2. It is seen that the II coefficient A_X depends on the applied electric field and on the width of the QW through the cross section of impact ionization. Our calculations within the electronic temperature model[32] indicate that the ionization coefficient is smaller for narrower wells. Thus, the experimental data confirm the theoretical predictions.[32]

As for the dependence of A_X on the electric field, a clarifying remark here is also in order. The analysis in Ref. 32 is based on hot electron temperature, which is a function of electric field strength. At stronger field, the hot carrier temperature is higher, therefore the increase of A_X with the field is expected. Obtained data exactly follow this prediction, i.e., A_X increases from 0.4 up to 10 cm^2/s for fields of 5–250 V/cm (QW of 20 nm width at temperature 77 K). At 4.2 K lattice temperature, somewhat higher values of A_X are obtained. However, we would like to stress that this approach is rather crude since the accuracy of the evaluation of the coefficient A_X is limited here mainly by the error in an initial free-electron concentration. Thus, in fact, Fig. 12 reflects the functional dependence, because the absolute scale of A_X can be inaccurate up to an order of magnitude.

Finally, it is worth noting that we have not observed a critical breakdown field for exciton impact ionization. For instance, for the QW of 20 nm width at 77 K, the field-induced breakdown starts at $F\geqslant 5$ V/cm, while at $T=4.2$ K it is around of $F\geqslant 20$ V/cm. The observed threshold was limited by the sensitivity of our experimental setup and more accurate measurements are needed. The decrease of the breakdown field with lattice temperature was explained earlier[37] with the help of the Boltzmann transport equation in the case of donor impact ionization. In general, the breakdown field depends on the balance between ionization and recombination, which have an opposite dependence on lattice temperature. Equation (8) shows that the strength of impact ionization depends on overlap of the distribution function $f(\epsilon)$ and exciton ionization cross section $\sigma_X(\epsilon)$. At temperatures close to liquid helium temperature, the overlap is negligible at zero electric field and finite at high electric fields. However, at high temperatures the overlap is finite even in the absence of electric field. As a result, the observed threshold field is lower at higher temperatures. From earlier theoretical considerations[32] it follow that no threshold breakdown field exists for excitons, when donors and acceptors are neglected.[38]

VI. CONCLUSIONS

In summary, we have examined the impact ionization processes in GaAs/$Al_{0.35}Ga_{0.65}As$ quantum wells in the electric field applied in-parallel to the layers. The PL quenching in dc electric field is studied at liquid helium and nitrogen temperatures and under different light excitation levels. First, we determined that the PL quenching of excitonic lines is related to the impact ionization of excitons and donors by electric field accelerated hot carriers. Second, the influence of the impact ionization of residual impurities on the quenching of excitonic photoluminescence is demonstrated: The impact ionization of neutral donors increases the concentration of electrons, which effectively recombine with holes on the acceptor levels; consequently, the decrease in the hole concentration diminishes exciton concentration since it is proportional to the product of electron and hole concentrations. Third, from the PL transients caused by the application of pulses of electric field of nanosecond duration, we determined that if the concentration of excited carriers is comparable with that of residual impurities, then exciton impact ionization by hot electrons can be time-resolved from donor impact ionization process. The first process was found to be very rapid and occurs within nanoseconds, while the second process with donors and acceptors is determined to be much longer, extending up to microseconds. Fourth, we developed the model for calculations of the photoluminescence tran-

sient shape and estimated the 2D coefficient of the exciton impact ionization, which was found to be in the range 0.4–20 cm^2/s at electric fields of 5–250 V/cm. In accordance with Ref. 32 we also determined that the 2D impact ionization coefficient increases with the electric field strength due to the mean carrier energy dependence on the applied in-plane electric field.

ACKNOWLEDGMENTS

This work was supported, in part, by Lithuanian State Science and Studies Foundation within the framework of ESPRIT Program Project PHANTOMS II ''Physics and Technology of Mesoscopic Systems'' and Lithuanian State Science and Studies Foundation Grant No. 20226.

*Present address: The State Service of Radio Frequencies, Algirdo 27, LT-2006 Vilnius, Lithuania.

[1] A. Dargys and J. Kundrotas, Lietuvos Fiz. Žurnalas **34**, 345 (1994) [Lith. Phys. J. **34**, 395 (1994)].

[2] H.-J. Polland, L. Schultheis, J. Kuhl, E.O. Göbel, and C.W. Tu, Phys. Rev. Lett. **55**, 2610 (1985).

[3] E.E. Mendez and F. Agulló-Rueda, J. Lumin. **44**, 223 (1989).

[4] J. Kavaliauskas, G. Krivaitė, A. Galickas, and I. Šimkienė, Lith. Phys. J. **36**, 140 (1996).

[5] E.E. Mendez, G. Bastard, L.L. Chang, L. Esaki, H. Morkoç, and R. Fischer, Phys. Rev. B **26**, 7101 (1982).

[6] K. Köhler, H.-J. Polland, L. Schultheis, and C.W. Tu, Phys. Rev. B **38**, 5496 (1988).

[7] G. Cohen and I. Bar-Joseph, Phys. Rev. B **46**, 9857 (1992).

[8] G. von Plessen, T. Meier, M. Koch, J. Feldmann, P. Thomas, S.W. Koch, E.O. Göbel, K.W. Goosen, J.M. Kuo, and R.F. Kopf, Phys. Rev. B **53**, 13 688 (1996).

[9] H. Weman, G.M. Treacy, H.P. Hjalmarson, K.K. Law, J.L. Merz, and A.C. Gossard, Phys. Rev. B **45**, 6263 (1992).

[10] M. Gurioli, J. Martinez-Pastor, M. Colocci, A. Bosacchi, S. Franchi, and L.C. Andreani, Phys. Rev. B **47**, 15 755 (1993).

[11] G. Oelgart, M. Proctor, D. Martin, F. Morier-Genaud, F.-K. Reinhart, B. Orschel, L.C. Andreani, and H. Rhan, Phys. Rev. B **49**, 10 456 (1994).

[12] Indeed, determination of the origin of these PL lines is complicated in this case due to the fact that the light-hole exciton (lh) ground-state energy ϵ_{lh} and the energy of the excited state of the heavy-hole exciton ϵ^*_{hh} are very close to each other. For instance, calculations with a 20 nm well indicate that $\epsilon_{lh}=6.65$ meV and $\epsilon^*_{hh}=5.88$ meV while the experiment gives the value $\epsilon_{exp}=6$ meV. For a 10 nm well these parameters are the following: $\epsilon_{lh}=16.3$ meV and $\epsilon^*_{hh}=8.06$ meV, while the experimental value ϵ_{exp} is about 12 meV. For a 5 nm well, ϵ_{lh} is 31.7 meV and ϵ^*_{hh} is 10.4 meV while ϵ_{exp} is 9 meV.

[13] G. Paulavičius, V.V. Mitin, and N.A. Bannov, J. Appl. Phys. **82**, 5580 (1997).

[14] C. Weisbuch, R. Dingle, A.C. Gossard, and W. Wiegmann, Solid State Commun. **38**, 709 (1981).

[15] G. Bastard, C. Delalande, M.H. Meynadier, P.M. Flijlink, and M. Voos, Phys. Rev. B **29**, 7042 (1984).

[16] C. Delalande, M.H. Meynadier, and M. Voos, Phys. Rev. B **31**, 2497 (1985).

[17] A. Čėsna, J. Kundrotas, and A. Dargys, J. Lumin. **78**, 157 (1998).

[18] B.K. Ridley, Phys. Rev. B **41**, 12 190 (1990).

[19] L. Pavesi and M. Guzzi, J. Appl. Phys. **75**, 4779 (1994).

[20] S.A. Solov'ev, Y.N. Yassievich, and V.M. Chistyakov, Fiz. Tekh. Poludrovodn. **29**, 1264 (1995) [Semiconductors **29**, 654 (1995)].

[21] A. Fujiwara, Y. Takahashi, S. Fukatsu, Y. Shiraki, and R. Ito, Phys. Rev. B **51**, 2291 (1995).

[22] A. Fujiwara, K. Muraki, S. Fukatsu, Y. Shiraki, and R. Ito, Phys. Rev. B **51**, 14 324 (1995).

[23] R. Kumar, A.S. Vengurlekar, S.S. Prabhu, J. Shah, and L.N. Pfeiffer, Phys. Rev. B **54**, 4891 (1996).

[24] R. Strobel, R. Eccleston, J. Kuhl, and K. Köhler, Phys. Rev. B **43**, 12 564 (1991).

[25] D. Robart, X. Marie, B. Baylac, T. Amand, M. Brousseau, G. Bacquet, G. Debart, R. Planel, and J.M. Gerard, Solid State Commun. **95**, 287 (1995).

[26] Zh.S. Asnina and L.G. Paritskii, Fiz. Tverd. Tela (Leningrad) **26**, 3300 (1984) [Sov. Phys. Solid State **26**, 1984 (1984)].

[27] R.L. Greene and K.K. Banaj, Solid State Commun. **53**, 1103 (1985).

[28] L.C. Andreani, F. Tassone, and F. Bassani, Solid State Commun. **77**, 641 (1991).

[29] J. Martinez-Pastor, A. Vinattieri, L. Carraresi, M. Colocci, Ph. Roussignol, and G. Weimann, Phys. Rev. B **47**, 10 456 (1993).

[30] D. Oberhauser, K.-H. Pantke, J.M. Hvam, G. Weimann, and K. Klingshirn, Phys. Rev. B **47**, 6827 (1993).

[31] J.H. Choo, Y.P. Feng, and H.N. Spector, J. Phys. Chem. Solids **55**, 1245 (1994).

[32] A. Dargys and J. Kundrotas, Semicond. Sci. Technol. **13**, 1258 (1998).

[33] M. Gurioli, A. Vinattieri, M. Colocci, C. Deparis, J. Massies, G. Neu, A. Bosacchi, and S. Franchi, Phys. Rev. B **44**, 3115 (1991).

[34] More specifically, donor-acceptor transition intensity is exponentially dependent on the distance between neutral donor and acceptor atoms. If transitions are time-dependent, the intensity of the PL cannot be described by a system of simple rate equations. How this problem can be solved partially may be found in Ref. 17.

[35] C. Weisbuch, in *Semiconductors and Semimetals*, edited by R. K. Willardson and A.C. Beer (Academic Press, New York, 1987), Vol. 24, pp. 1–33.

[36] J. Kundrotas, Semicond. Sci. Technol. **14**, 461 (1999).

[37] A. Dargys and J. Kundrotas, Solid-State Electron. **41**, 1185 (1997).

[38] Threshold breakdown field is usually evaluated from the stationary electron concentration as a function of recombination and impact ionization coefficients.[1] In the idealized model of Ref. 32, where the concentrations n_X and $n=p$ are taken into account only, at all electric fields the linear relation between concentrations was found: $n(E)=an_X(E)+b$, where $a>0$ and $b>0$ are constants, independent of impact ionization. This relation gives no critical breakdown field.